DIFFRACTION OF MICROWAVES

DIFFRACTION OF 3.2 cm MICROWAVES BY A CONDUCTING

AND A

DIELECTRIC ROD WITH DIAMETER OF THE ORDER OF

A WAVE-LENGTH

By

SYDNEY THOMAS WILES, B.Sc.

A Thesis

Submitted to the Faculty of Arts and Science

in Partial Fulfilment of the Requirements

for the Degree

Master of Science

McMaster University

October 1952

TITLE: Diffraction of 3.2 cm Microwaves by a Conducting
           and a Dielectric Rod with Diameter of the Order
           of a Wave-Length.

AUTHOR: Sydney Thomas Wiles   B.Sc. (McMaster)

SUPERVISOR: Professor A. B. McLay

NUMBER OF PAGES: 33

SCOPE AND CONTENTS:

        A description of the apparatus used in microwave
phase and diffraction measurements is contained in the first
chapter of this thesis. The field was investigated by a
phase technique and the point source of radiation reasonably
well established. Several diffraction patterns about a
dielectric and a conducting rod were taken at several dis-
tances behind the rod with the E vector of the field
parallel to the axis of the rod. These were qualitatively
analysed and compared with the patterns of one other worker
at 1.25 cm. Agreements and differences were noted.

ACKNOWLEDGEMENTS

TABLE OF CONTENTS

LIST OF ILLUSTRATIONS

CHAPTER I

INTRODUCTION.

THE USE OF ELECTROMAGNETIC WAVES FOR THE STUDY OF DIFFRAC-
TION

Electromagnetic waves are the phenomenon by which
energy may be transmitted from one point in space, occupied
by a suitable generator to another remote point where the
intervening distance may be occupied by various substances
called dielectrics or by "free space". In "free space"
these waves travel with a constant velocity c, which is
usually called "the velocity of light" and which is another
one of the universal physical constants. However, when
this energy is being propogated through a material medium
other than "free space" the velocity of propogation v is
always smaller numerically than c. To describe accurately
the nature of the electromagnetic disturbance, both the
frequency of the oscillation, which is a property of the
source and the wave-length of the wave itself are used.
These are related by $v = \nu\lambda$. When the whole spectrum of elec-
tromagnetic waves is considered, the wave-length has been
found to vary from the order of 10^{-10} cm in the highly energe-
tic cosmic and gamma ray region down through the sections
denoted the X-ray, ultraviolet, visible and infra-red to the
long radio wave regions. Diffraction affects in the visible
light region are familiar, but the actual dimensions of the

-1-

apparatus and the wave-length used incur limitations when
it comes to investigating the phenomenon of diffraction close
to the objects from which this diffraction arises since the
wave-length of the radiation is very small compared with the
dimensions of ordinary objects. Until recent years, the gap
between long light waves and short radio waves was large.
To arrange for measurements of diffraction of radio waves
would require apparatus and laboratories prohibitively large.
With the coming of ultra high frequency oscillators which
utilize the oscillations of electrons in a confined
macroscopic field space, it is possible to obtain electro-
magnetic waves with wave-length between 10^{-1} and 10^{2} cm.
Thus the study of diffraction was extended to that close to
obstacles and also to obstacles with dimensions of the order
of the wave length.

It should be noted that electromagnetic waves in this
microwave region provide "one of the most perfect examples of
the application of Maxwell's equations" [1] which, when sub-
jected to the appropriate boundary conditions are sufficient
to describe the behavior of the radiation in the problem under
consideration. For a careful account of the nature of
electromagnetic waves, the reader is referred to Chapter 1
of the thesis submitted by D. B. McLay for the degree of
Master of Science, 1951.

This worker is familiar with the limitations im-
posed by McLay's set up and steps taken to improve them will
be outlined. Taking point to point readings as in the previous

work consumed much time and when a complete diffraction run was completed it was noted that the intensity of radiation from the source had changed in the time interval between the start and stop of the run. Particularly since the study of the whole field could not be completed in the space of a day this variation made it difficult to relate the results of one day's work to those of the next. And so, it was decided to use a more rapid continuously recording setup which would provide a means of moving the energy measuring device at a uniform speed in the desired direction.

The generator used was a klystron oscillator which provided radiation with frequency between 7,000 and 10,000 mc/s and the wave length chosen was 3.20 cm. Since the output of the generator was of the order of a few milliwatts as opposed to the 40 watts continuous beamed power of McLay's radar source, (magnetron) it was necessary to build a stable ac amplifier with a voltage gain of around 40,000. With these changes it was possible to perform the whole diffraction experiment in the space of 5 hours. Coupled with the fact that the output of the klystron generator was intrinsically more stable than that of the radar source, this made it possible to relate the results of the whole field, not only from the standpoint of maxima and minima positions, but also from the point of view of the relative intensities of all the diffraction patterns observed.

Experiments were begun in the Nuclear Research Build-

ing in a room with dimensions about 10 x 10 meters, but inter-
ference caused by various equipment and limitations of space
led to the moving of the apparatus to a larger laboratory
with dimensions 10 x 18 meters where electrical interference
was considerably less.

Reference:

1.   J. C. Slater and N. R. Frank, Electromagnetism,
        (New York, McGraw-Hill Co. 1947)

CHAPTER II

THE EXPERIMENTAL EQUIPMENT

(1) THE MICROWAVE GENERATOR

The microwave generator was built by D. B. McLay and
D. G. Inch as a B.Sc. problem. The circuit diagram and oper-
ating information for it are covered in the references.[2]
Basically, the klystron is a cavity oscillator which utilizes
the oscillations of electrons in the space between the
cathode and the reflector of the tube and the frequency of
oscillation of the electrons is governed by the dimensions of
the cavity itself, and by the voltages of the anode, grid and
particularly the reflector. Since the klystron is so voltage
dependent, a well regulated power supply is necessary. To
obtain this, the reflector voltage is controlled by a 6Y6G
regulator tube and 6SJ7 control tube, and may be varied from
15V to -210v with respect to ground. The klystron anode is
grounded and since the tip anode potential is 200v to 300v,
and the reflector voltage is -15v to -210v, a total drop
across the tube of 510v is obtained, while keeping the tube
case, and therefore, the waveguide assembly at ground poten-
tial. The modulator is a square wave generator whose output
is variably coupled to either the reflector or the grid of the
klystron. For these experiments, reflector modulation was
used since it produced a minimum of frequency modulation.
The action of the modulator in this case may be seen by con-
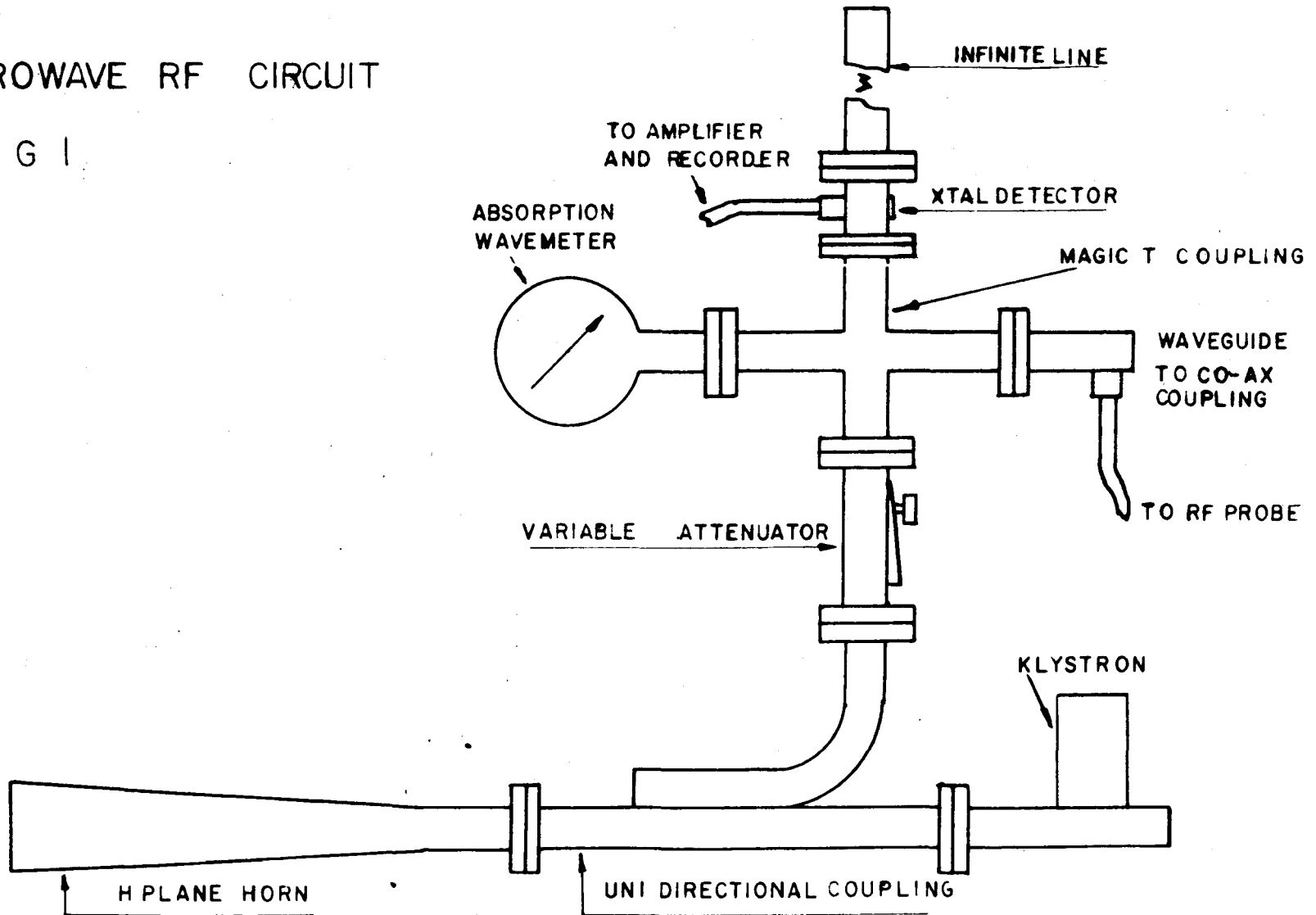sidering Fig. 16a. The same frequency of oscillation may be

-5-

obtained at several reflector voltages when all other conditions including the tuning of the resonator are kept fixed. Each of these corresponds to a different number of cycles of drift of the electrons in the reflector space, and this characteristic is illustrated in Fig 16(a), which shows approximately the relative output as a function of the reflector voltage, for various mean resonator frequencies obtained by mechanically tuning the klystron. Operation for phase measurements to be discussed later was chosen in mode A because it afforded greatest output, while for diffraction measurements either mode B or C was chosen to reduce the field intensity. This was found necessary because if the field intensity were low, the contribution of stray effects to disturbing the field was less than for larger fields. Suppose that the oscillator is running at the operating point marked A in Fig 16 (a). If the reflector voltage is varied along the line A B by a superimposed square wave, the klystron may be switched from an oscillating to a non oscillating condition. If A lies at the top of the "hump" or on the left side of it for a negative going square wave, there is no frequency modulation. However, if A is on the right side of the "hump" or if A B is not flat, and the top of the square wave not constant, there will be frequency modulation of as much as 20 to 30 mc/s on each cycle, and a corresponding shift in wave-length. Now, if the wave-length varies from 3.200 cm to 3.215 cm due to this 30 mc s shift, there is a shift of half a wave-length of the end of a wave guide run, or path in free space of only 100

wave-lengths. Obviously, this would be disastrous in phase measurements, which will be described later where the total distance travelled by the rf energy was of the order of 150 wave-lengths. And so, it can be seen that a klystron may be amplitude modulated if A is on the left side of the "hump", by applying a square wave to the reflector, and it is this square wave envelope, obtained from a crystal detector, that is amplified and recorded by the remainder of the apparatus.

It requires extreme care in adjustment of the controls of this generator to obtain optimum results from it. First of all, adjustment of the klystron frequency will be considered. As it has been pointed out before, the most important factorsin deciding the klystron frequency are the physical size of the resonator cavity and the value V_r of the voltage on the reflector, and so, a definite tuning procedure must be used. Some means of monitoring the output must be used also and this is a crystal diode, held in an appropriate wave-guide mounting, with output fed to an oscilloscope which is swept to show the square wave pattern. The klystron is then tuned mechanically to approximately the proper frequency as shown by an absorption wave meter used in conjunction with the crystal diode (fig 1) and the bows of the klystron are then flexed a number of times to relax the strain on the cavity diaphram. By decreasing the flexing successively from a maximum of one full turn to zero in eight or ten flexes, the desired frequency will be essentially stable from a mechanical standpoint. The next step is to adjust V_r for maxi-

MICROWAVE RF CIRCUIT

FIG 1

INFINITE LINE

TO AMPLIFIER
AND RECORDER

XTAL DETECTOR

ABSORPTION
WAVEMETER

MAGIC T COUPLING

WAVEGUIDE
TO CO-AX
COUPLING

TO RF PROBE

VARIABLE   ATTENUATOR

KLYSTRON

H PLANE HORN

UNI DIRECTIONAL COUPLING

mum output in the desired mode (determined by wave meter and fig 16(a). This will change the frequency of oscillation and it will have to be corrected by a slight adjustment of the mechanical tuning. This procedure is repeated several times until a maximum output at the desired frequency is obtained. This combination of mechanical tuning shifts the positions of the "humps" in the various modes and this allows adjustment of the operating point to the peak of one of these "humps". Thus, when the klyston is modulated, it will be done along the line AB of fig 16(a) and frequency modulation will be a minimum. It should be noted that the penetration of the klystron probe in the waveguide system changes the loading of the oscillator and hence the output frequency, and so this adjustment should be made with care. For lower output, one of the other modes should be selected and in this case, tuning is essentially the same. The greatest power output of the 723 A/B klystron is 20 milliwatts.

(2) THE AMPLIFIER AND ITS POWER SUPPLY

Since the power output of the generator is small as compared with the power used in the radar source in the previous work at this university, [4] it was necessary to build a high gain amplifier (fig 2) to amplify the energy picked up by the probe so that the recording apparatus could be used. The amplifier is a standard r-c coupled one with three tetrode stages. It was found necessary to incorporate the decoupling devices C_7 and R_{10}, C_8 and R_{11} which effectively decrease the
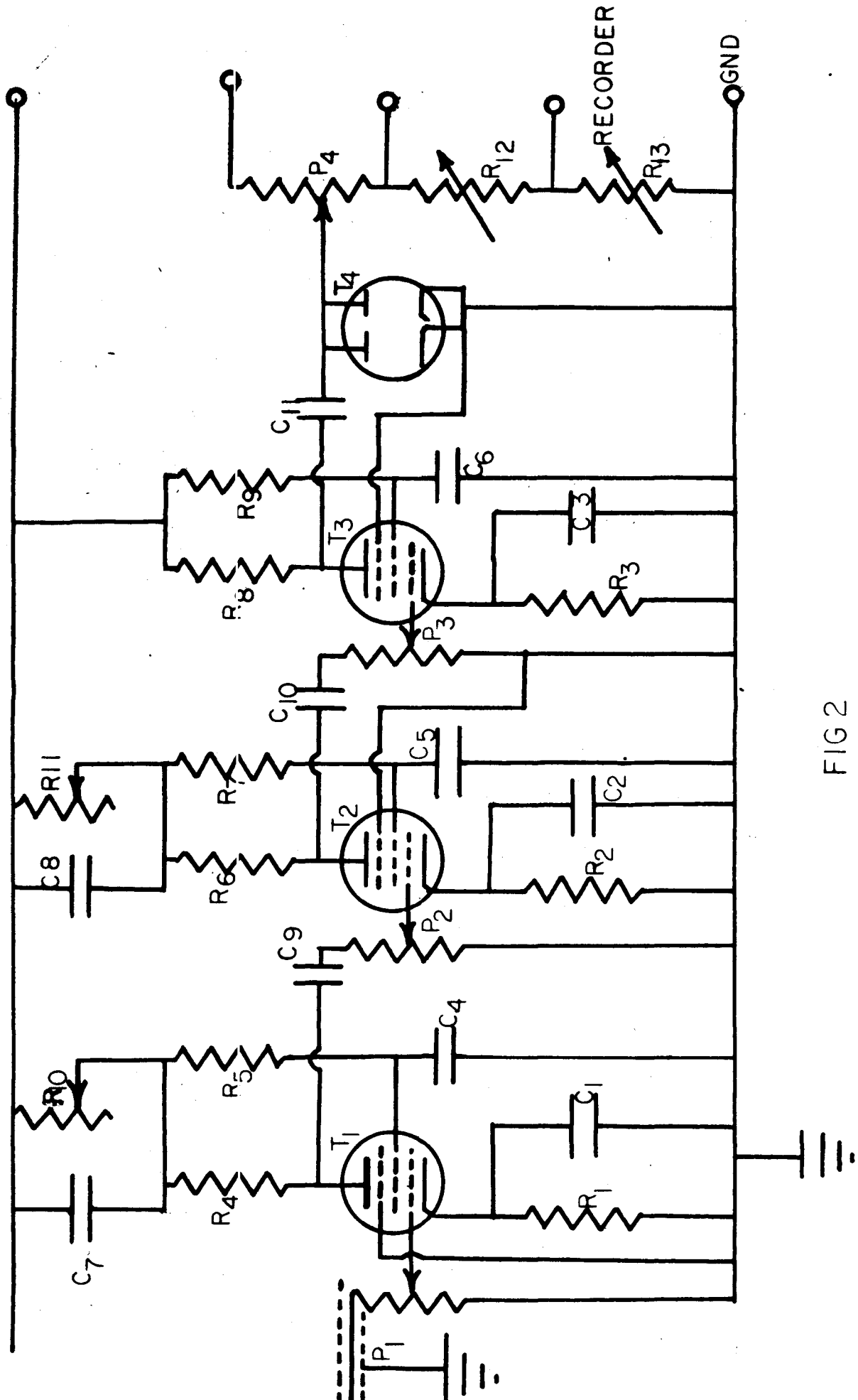
FIG 2

amplitude of the signal across the plate load resisters R_4 and R_6, so that motorboating or self oscillation could be overcome. The amplifier was operated from a rebuilt IFF (radar) power supply [5] which delivers 255 volts regulated, 200-300 volts variable regulated, and 6.3 volts a.c. for filaments. Because of the high gain of the amplifier it was necessary to add an additional condenser input filter with 80 mfd, 10 henries, and to keep the power supply remote from the amplifier, feeding the HT through a co-axial cable. To eliminate interstage coupling and ac filament pickup, each stage was separated and shielded completely and the filaments operated on 6.3 volts dc. Fig 3 shows the dependence of the amplifier on filament voltage and ac line voltage was operated at 115 volts, 60 c s, and the filaments at 6.3 - 0.1 volts d. c. The voltage gain of the amplifier was nearly constant at around 35,000 up to a signal input of 0.6 millivolts, when it dropped rather sharply to about 25,000. However, the signal input from the crystal detector was of the order of several microvolts and so any appreciable change in gain would not occur. The amplifier itself was not entirely ideal in this respect and much improvement can be made. Some workers in this field have used narrow band amplifiers but this wide band circuit was chosen because minimum distortion of the square wave output of the detector was desired. Moreover, little is known in this laboratory about the change in gain due to distortion of the square wave by a narrow band amplifier.
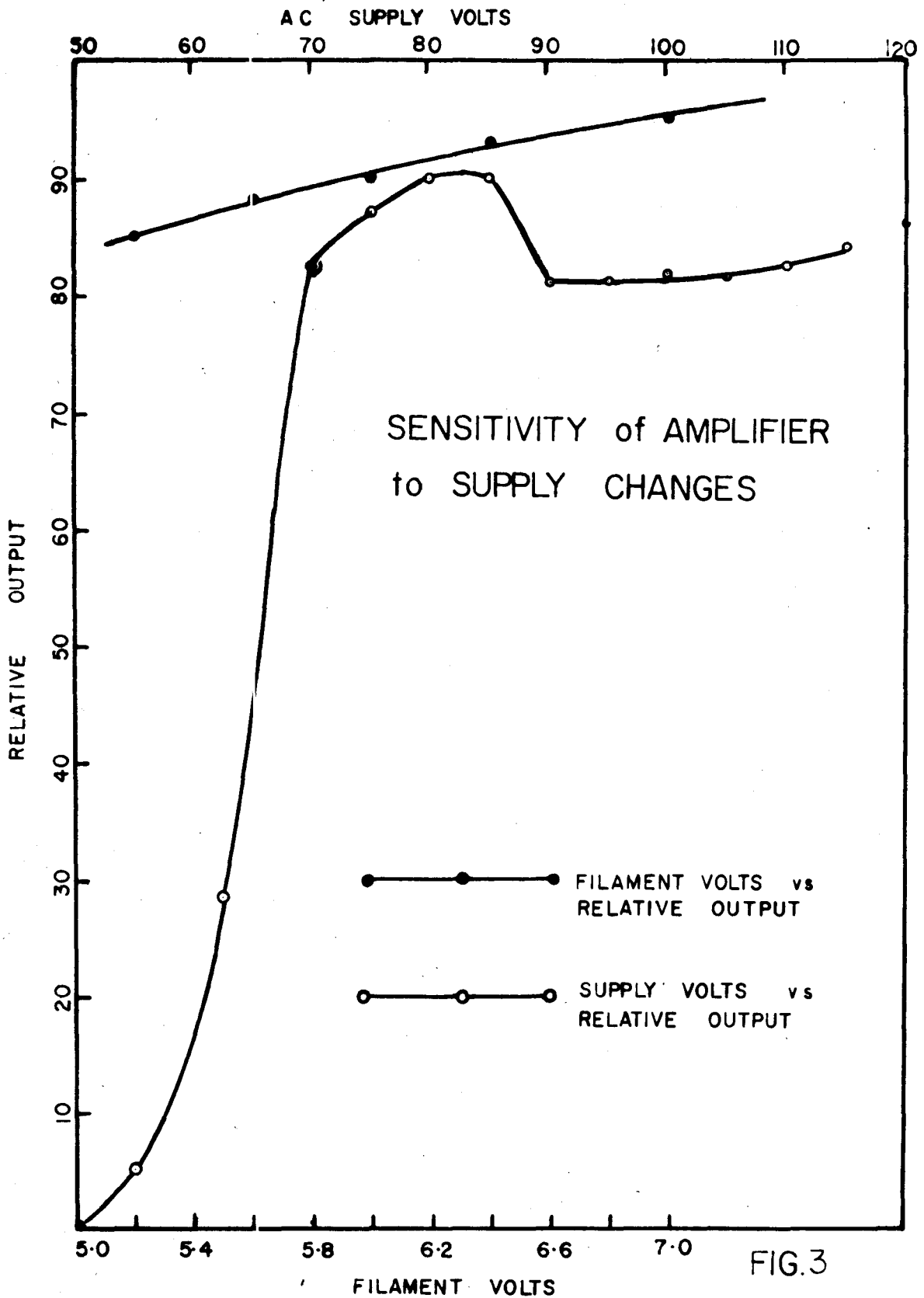
FIG.3

Since the recorder used was a d c voltage instrument with a full scale deflection of 5 millivolts, the output of the amplifier was clamped by a 6H6 diode, sections connected in parallel, to a d c level set by a 45 volt battery across P_4 (1 meg). This d c level was adjusted so that with zero input from the probe in the field, the recorder would read approximately zero, that is, the internal noise of the amplifier was cancelled out, leaving only the desired signal from the probe in the field.

(3) THE RECORDER BALANCE NETWORK

The resistor combination P_4, R_{12} and R_{13} in Fig 2 constitutes the recorder balance and load network. The input resistance to the recorder must not exceed 250 ohms and so some means had both to provide a load across which the d c output of the amplifier could be applied to the recorder, and to allow the recorder to be balanced down to a reference zero. The noise of the amplifier was nearly constant and when rectified provided a steady but undesirable d c level. This was balanced out by a voltage applied across P_4 in the proper sense. A load is provided by R_{12} and R_{13}, the latter of which is kept below 250 ohms.

(4) THE RECORDER

The recorder is a Brown Electronik instrument, manufactured by Minneapolis Honeywell Company. The chart was divided by a 0 - 100 scale and was driven at 2" per minute

for all records. One general drawback of the instrument was the fact that the recorder had a $4\frac{1}{2}$ second maximum scale response, and this imposed a limit on the maximum probe speed. When the track was driven at 1 mm per second the recorder would distort the low intensity minima near zero.

It should be noted that the case of the instrument is normally grounded and the centre input conductor is positive. Now if it is recalled that the amplifier output is fed to the plates of the 6H6 clamp tube it is obvious that the output across the recorder load resistor (R13, Fig 2) will be negative at the top end. It proved to be impossible to hold the cathodes at the output potential with the plates grounded because the filaments would then transfer any pickup which largely 25 c/s hum to the cathodes and thence to the recorder. Thus it was necessary to run the recorder with the inside input terminal grounded and the case at negative potential on the 6H6 plate side of R_{13}. However, this did not cause any increase in the d c noise level of the recorder because even though pickup by the instrument might be rectified by the diode and applied across the recording circuit in the proper sense, it would not be amplified and hence could be neglected.

(5)   THE MICROWAVE RF CIRCUIT

This circuit is the means by which the field could be set up for phase and intensity measurements. Reference is made to Fig 1 and Ref. 3, pg 915.

The microwave radiation originated in the 723 A/B

klystron, which is coupled to the waveguide by a probe. This radiation passed through the undirectional coupling, which allows a small amount of energy to flow back from the vertical components to the main waveguide run made up of the oscillator, coupling and horn. A large part of the radiation passed through the coupling on into the H-plane horn. The horn is 90 cm long, front edge to apex, and measures 28.2 cm along the front edge. In other words, the horn is flared with a flare angle of 52° in the plane of the wide dimension of the waveguide and concentrates the energy in horizontal sense, with the electric vector vertical. The wave fronts, therefore, resemble right circular cylinders, orientated with the axis of the cylinder vertical. Failing a plane wave front, this is the most ideal form of radiation for studying diffraction about cylinders. In the microwave field, the energy is picked up by a tuned crystal diode probe, Fig 4, for intensity measurements and is then amplified and recorded by the appropriate apparatus described previously.

The wave-length is monitored by the absorption wavemeter mounted on one arm of the "magic T". The output of this detector was fed to the monitor scope through its preamplifier. The wavemeter is a tuned resonant cavity that absorbs energy when tuned to resonance at the incoming wavelength and hence indication of its being tuned is a sharp drop in the amplitude of the signal on the monitor screen. The wavemeter reads directly in frequency and has a range from 9285 to 9465 mc/s (9375 mc/s = 3.2 cm) and a sensitivity of $\pm$ 1 mc/s.

DIAGRAM OF CRYSTAL DIPOLE PROBE

HARD RUBBER ROD, 10 λ LONG

SIDE VIEW

END VIEW

0.25 cm

2.54 cm

1.6 cm

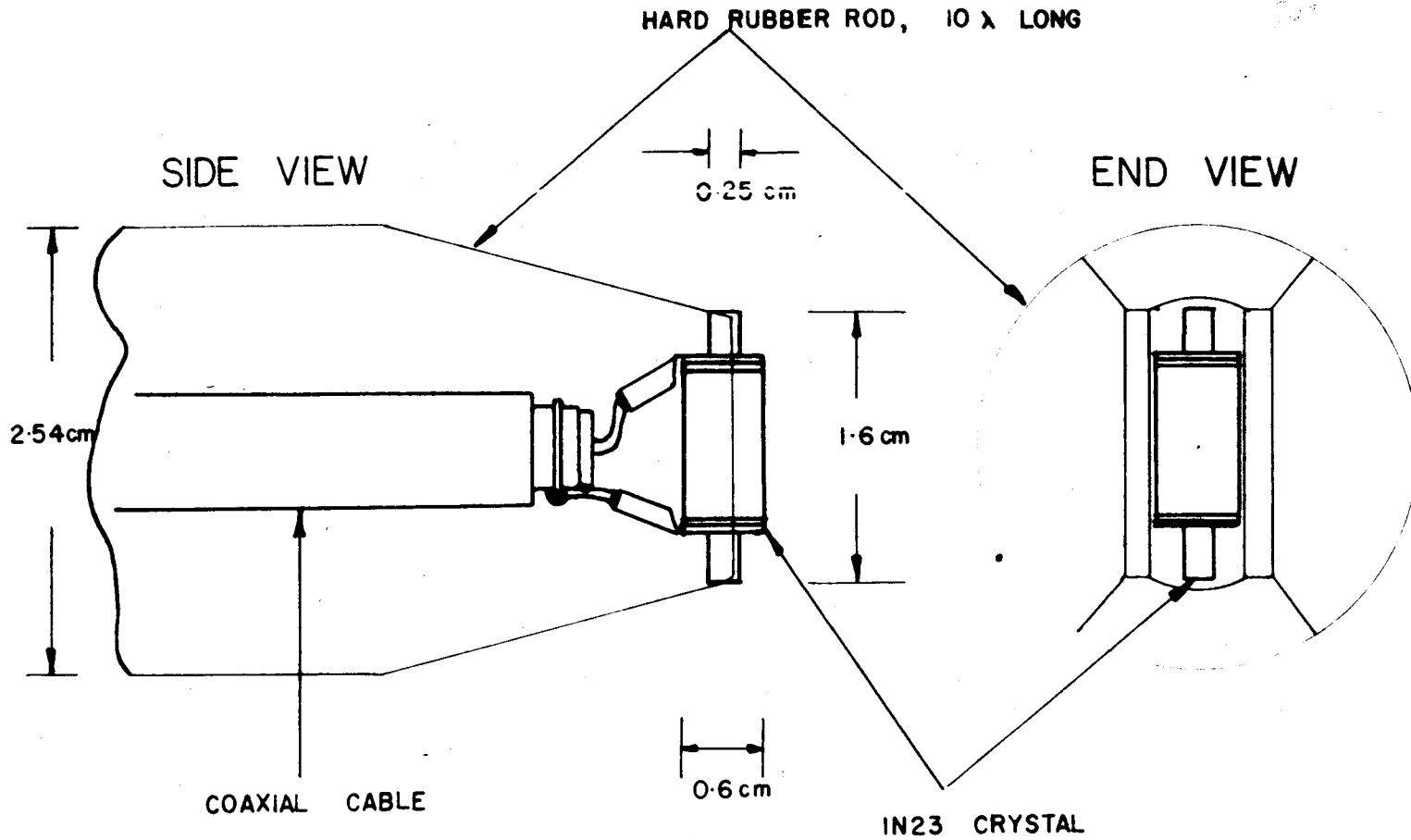COAXIAL CABLE

0.6 cm

IN23 CRYSTAL

FIG. 4

For measurements of phase change in the field, the same setup was used in a different sense. The probe in this case is an rf one which picks up the microwave energy and feeds it via a co-axial cable, fitted with low loss couplings to the right hand arm of the "magic T". The amazing fact is that 10,000 m c/s energy will pass through a co-axial cable, although attenuation is quite high and this fact imposes a limitation on the use of the apparatus. A far more suitable arrangement would be a waveguide run with flexible couplings from the track to the "magic T", a distance of approximately 4 meters, but the distance made this arrangement impracticable at the time. The amplifier and recorder are then fed from the crystal detector in the waveguide section immediately above the "magic T" coupling.

To understand the function of the circuit when used for phase measurements, one must consider radiation travelling by two paths, one of which is fixed and the other variable in length. The fixed path is the one from the klystron, up through the unidirectional coupling, the variable attenuator, through the "magic T", past the crystal detector and thence on up into the infinite line where the radiation is "lost". This path is fixed for a given setting of the klystron and provides the reference signal. The second is from the klystron, on out through the coupling and horn to space where the signal is picked up by the probe and fed back via the co-axial cable, to the right hand arm of the "magic T" and mixes with the reference signal. These two signals will interfere construc-

tively or destructively depending on the path length, or
change in path length of the second described signal. Thus,
variation of intensity is produced at the crystal detector
and this constitutes the phase signal which is amplified
and recorded. As mentioned before, the attenuation of the
signal by the co-axial cable, and further, the efficiency of
the rf probe are governing factors in the extent to which
the apparatus may be used. Care must be taken that the
reference signal and the rf probe output are nearly of the
same magnitude; the reference signal being slightly larger.

This leads to a discussion of the probes themselves.
The rf probe (fig 5)[6] is basically a matched half-wave
dipole, and careful experiments were performed to provide
the best probe. The results of these experiments are given
by the curves in fig 6, and they show the relation between
the balancing slot length and the dipole length, as well as
the length of the matched dipole and the relative output of
the probe for constant field intensity. The experiment was
performed by varying the dipole length from 5.0 to 1.0 cm,
and for each of these dipoles, varying the slot length from
1.0 to 0.0 cm, recording the relative output for each setting.
All variations were made in mm steps. The curve Dipole
Length vs. Slot Length (fig 6) was obtained by plotting the
slot length for maximum output readings against the corres-
ponding dipole length. This explains the seemingly step-
wise nature of the curve. The experiment was then performed
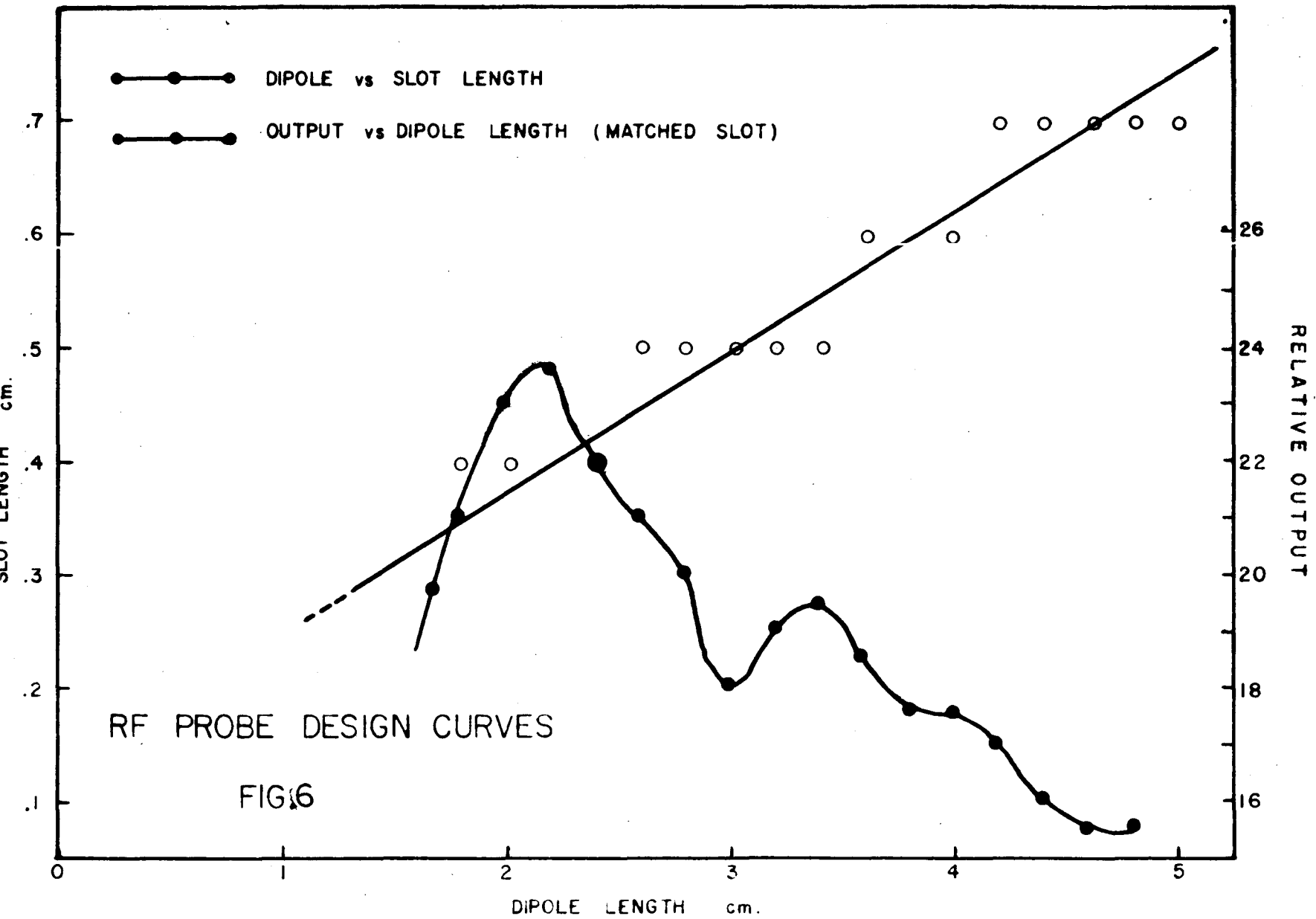by varying the dipole length, adjusting the slot length

DETAIL RF PROBE

2·14

0·39

4·0

0·85

0·005" Cu
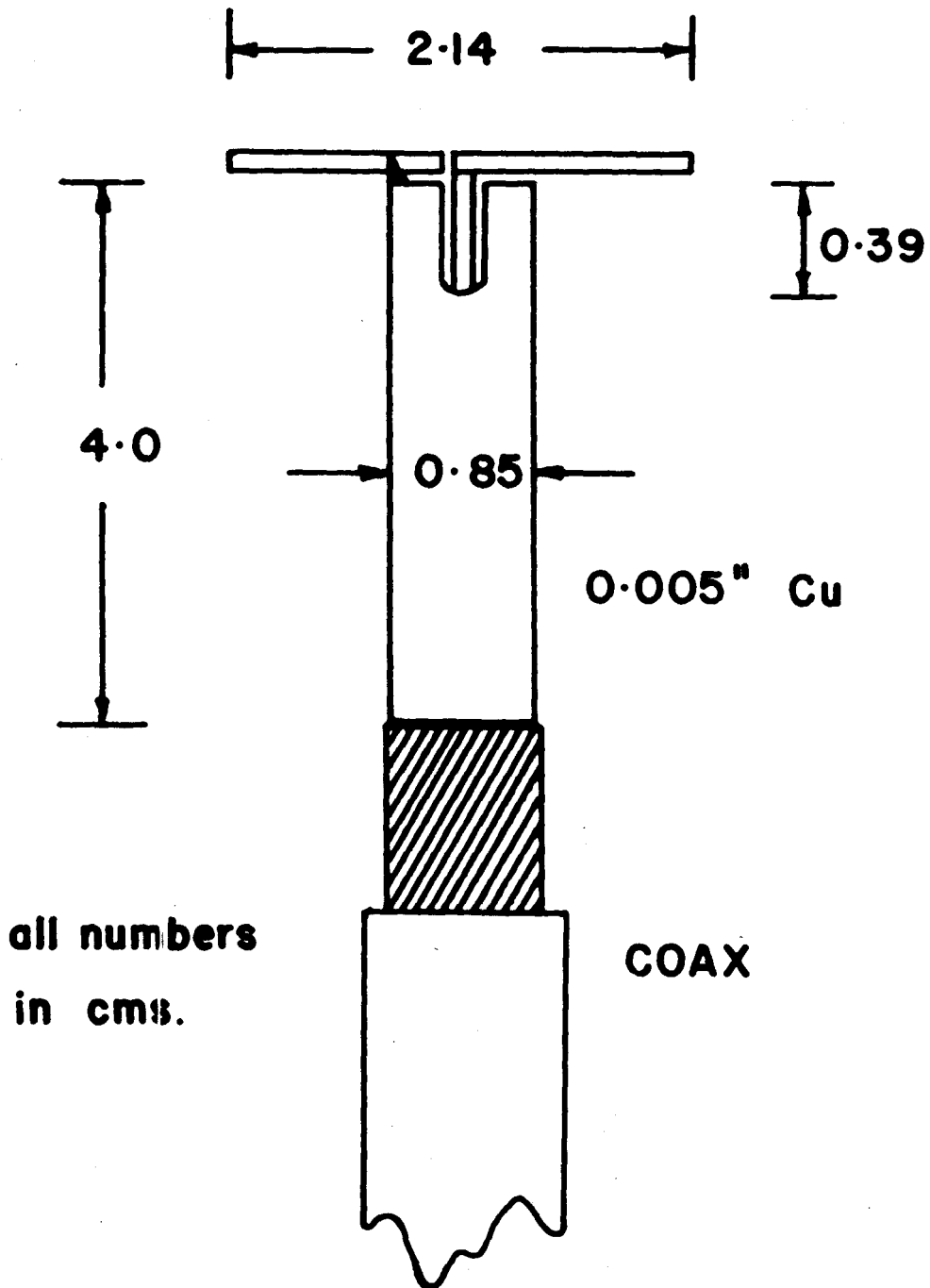
all numbers
in cms.

COAX

FIG 5

RF PROBE DESIGN CURVES

FIG.6

according to the previous curve, and recording the relative output of the probe. It was found that not only the slot and dipole lengths are variables for a given setup, but also the diameter of the cable used. These measurements hold for a cable whose sheath diameter is 0.85 cm.

The crystal diode probe[10] was a IN23A diode, turned down to the dimensions shown in Fig 4. For the field intensities used, it is essentially a square law detector, and is the same as described in ref 4, with the exception that the crystal was cut to $0.98\lambda/2$ for greater signal output. It is felt that reradiation from the crystal is negligible because oscillations would be severely damped by the back to front ratio of the crystal (approximately 100:1).

(6) STABILITY TESTS

The frequency stability of the oscillator was of prime concern, as has been mentioned before, and it was decided to perform some tests to determine whether or not external influences could be causing any "pulling" of frequency.

In the phase measurements it was considered possible that some of the reference signal could be re-radiated by the probe and cause an interference pattern in the main waveguide run. It was also thought that some energy could be flowing backwards through the unidirectional coupling. To determine whether or not this was so the crystal detector was inserted in the main waveguide run, and a phase experiment performed. With the amplifier gains wide open, and recorder adjusted to

maximum sensitivity, no interference pattern was observed. Hence this possibility was ruled out. Next the absorption wavemeter and crystal detector were inserted in the main waveguide run and the wavemeter was adjusted so that the signal on the amplifier monitor was midway between steady reading and minimum indication. That is, the wavemeter was adjusted so that its resonant frequency was just to one side of the oscillator frequency. Any shift in oscillator frequency towards the wavemeter resonant frequency would cause an increase in the recorder indication, and conversely, any drift away from the wavemeter frequency would cause a decrease in the indication. This is in effect a frequency detector and will determine any drift of the oscillator frequency. First the apparatus was held constant while the recorder was run over a period of an hour. It was found that the frequency of oscillation did not vary by more than one megacycle per second. Next, by moving the probe in the direction of the field, it was found that the frequency of oscillation was independent of the probe position. As a result of these stability tests it can be said that the frequency of the oscillator was independent of external influences to better than one part in 10,000. It was found however, that air currents across the klystron would cause drifts of the order of 20 mc.

(7)   TRACK AND PROBE ASSEMBLY

By means of the assembly shown in fig 7 the probes are moved along the field in the desired direction. The
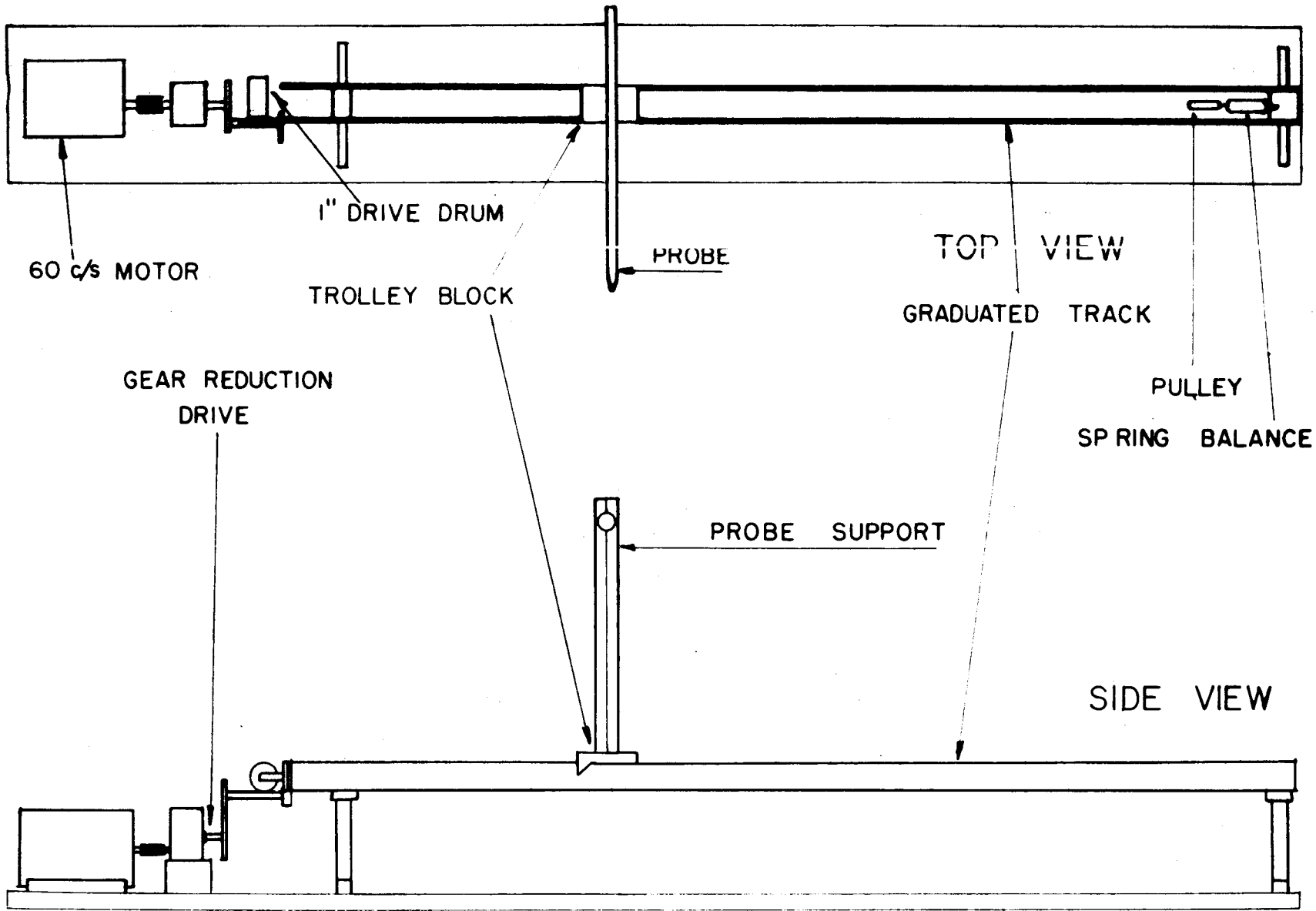
I" DRIVE DRUM

PROBE

TOP VIEW

60 c/s MOTOR

TROLLEY BLOCK

GRADUATED TRACK

PULLEY

SPRING BALANCE

GEAR REDUCTION
DRIVE

PROBE SUPPORT

SIDE VIEW

TRACK AND PROBE ASSEMBLY

FIG 7

driving power is obtained from a 3600 r.p.m. ac motor geared down by means of a 9900:1 worm reduction box which turns a 1" diameter drum. A continuous stranded cable is wound three times around this drum and passes over a pulley which is kept under 14 lbs tension by a spring balance at the other end of the track. The track is an optical bench which supports a grooved block. This block, which carries the stand holding the probe rod is fastened to the cable already described. The probe rod is approximately 25λ above the floor and 20λ in front of the track. The probe is driven along the track at approximately 1 mm/sec in either direction. While the recorder chart was operated by a synchronous motor and the probe by an induction motor, it was found that their motions remained reasonably well locked to better than one part in five hundred.

References

2.   Operating Information, #108, Klystron Power Supply and Square Wave Modulator 7VN-7BL.

4.   D.B. McLay, Thesis for degree Master of Science, McMaster University, 1951.

5.   Operating Information #113, IFF Power Supply.

6.   D. W. Fry and F. K. Goward, Aerials for centimetre Wave-Lengths, Cambridge University Press, 1950, pg 45.

10.   C. L. Andrews, J. Appl. Phys., 21, 764, (1950).

CHAPTER 3

DIFFRACTION OF 3.2 cm WAVES

(1)   PHASE MEASUREMENTS OF THE FIELD

Since the interpretation of diffraction affects in-
volves a knowledge of the exact position of the source of rad-
iation, it was necessary to determine experimentally the
effective source position in the horn. This was done by deter-
mining the phase changes in the field at various distances
from the horn, and computing the effective source position as
described below. The method of measuring phase shifts has al-
ready been described in Chapter 2, section 5.

Assume that the wave fronts are cylindrical. Consider
fig 9. Each one of the curves, W_1, W_2, W_3, $\cdots$, W_n, represents
wave fronts differing in phase by one or more whole wave-
lengths. If one draws a line perpendicular to the axis of the
field SX, denoted by YZ, the distances X_1, X_2, X_3, $\cdots$, X_n
represent the distances from the axis SX to the intersections
of YZ with the wave fronts W_1, W_2, W_3, $\cdots$, W_n at A,B,C,D, $\cdots$.
If the phase of the wave arriving at W_1 is such that construc-
tive interference occurs at the crystal detector in the ver-
tical waveguide run (fig 1), the indication on the recorder will
be a maximum. As the probe moves along YZ, maximum indica-
tions will be obtained at A, B, C, and so on. The maximum at
B represents the distance of A from S plus one wave-length,
and the maximum at C represents the distance of A from S plus
two wave-lengths, and so on. By comparing triangles

$$\sqrt{(R + [n-1]\lambda)^2 - X_n^2} = \sqrt{R^2 - X_1^2}$$
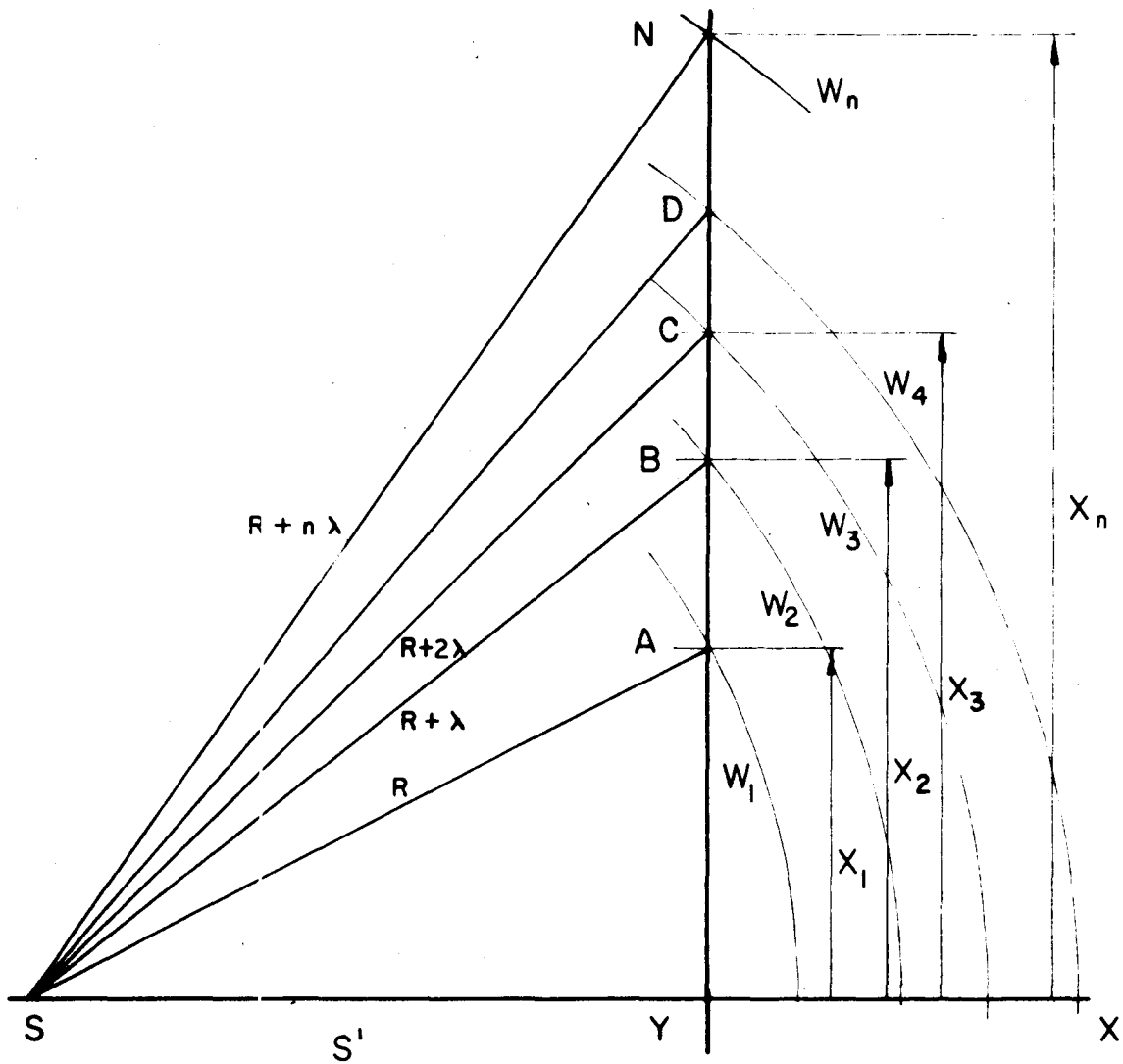
DIAGRAM FOR FIELD SOURCE DETERMINATION

FIG. 9

and solving

$$R = \frac{X_n^2 - X_1^2 - (N-1)^2 \lambda^2}{(n-1)} \qquad (1)$$

also

$$S' = \sqrt{R^2 - X_1^2}$$

where $n-1 = 1,2,3, \cdots$ represents the number of the maximum $A, B, C, \cdots$.

Fig 16 (b) is a sample curve for these measurements, and the foot-note shows a sample calculation.

Footnote

Sample field calculation.

$X_1 = 18.7$ cm	$X_1^2 = 352$
$X_2 = 32.3$	$X_2^2 = 1043$
$X_3 = 41.1$	$X_3^2 = 1687$
$X_4 = 48.7$	$X_4^2 = 2565$

From Equation (1)

$R = 106.4$ cm	$S^* = 104.5$ cm
and 101.0	$= 100.0$ cm
and 112.0	$= 110.0$

Since the field is assumed circular S^* is averaged.

   $S^*_{av} = 105.5$ cm

Probe distance from the front of the horn = 68.3 cm

   $S' = 105.5-68.3 = 37.2$ cm.

The results of the whole series of experiments are
illustrated by fig 8, where the distance of the source from
the front of the horn is plotted against the distance of the
probe in front of the same edge. The curve shows that the
apparent source position is a function of the distance of the
probe from the apex of the horn (60 cm). For small distances
the source is considerably in front of the apex, but for dis-
tances greater than 300 cm, such as were used in these experi-
ments, it appears to be essentially at the apex. The fact
that the apparent source changes may be due to two reasons.
First, the dipole may re-radiate energy and thus by its
presence, influence the virtual source. However, this does
not seem likely since it was found previously that the probe
had little influence on the conditions of the oscillator.
Secondly, the wave fronts in the field itself are not
cylindrical (circular) as assumed, but rather are more ellip-
tical in shape with the major axis along the axis of propoga-
tion. When the probe is close to the horn, a larger number
of maxima are noted, than is the case when the probe is more
distant. For these short positions the assumption of cir-
cular cylindrical wave fronts is certainly not valid. On the
other hand, errors at greater distances are increased because
energy arriving at the probe may travel by various other in-
direct paths, particularly by reflection from the floor, and
affect the phase at each point in the wave. This together
with the fact that the wave fronts are more tangential to the
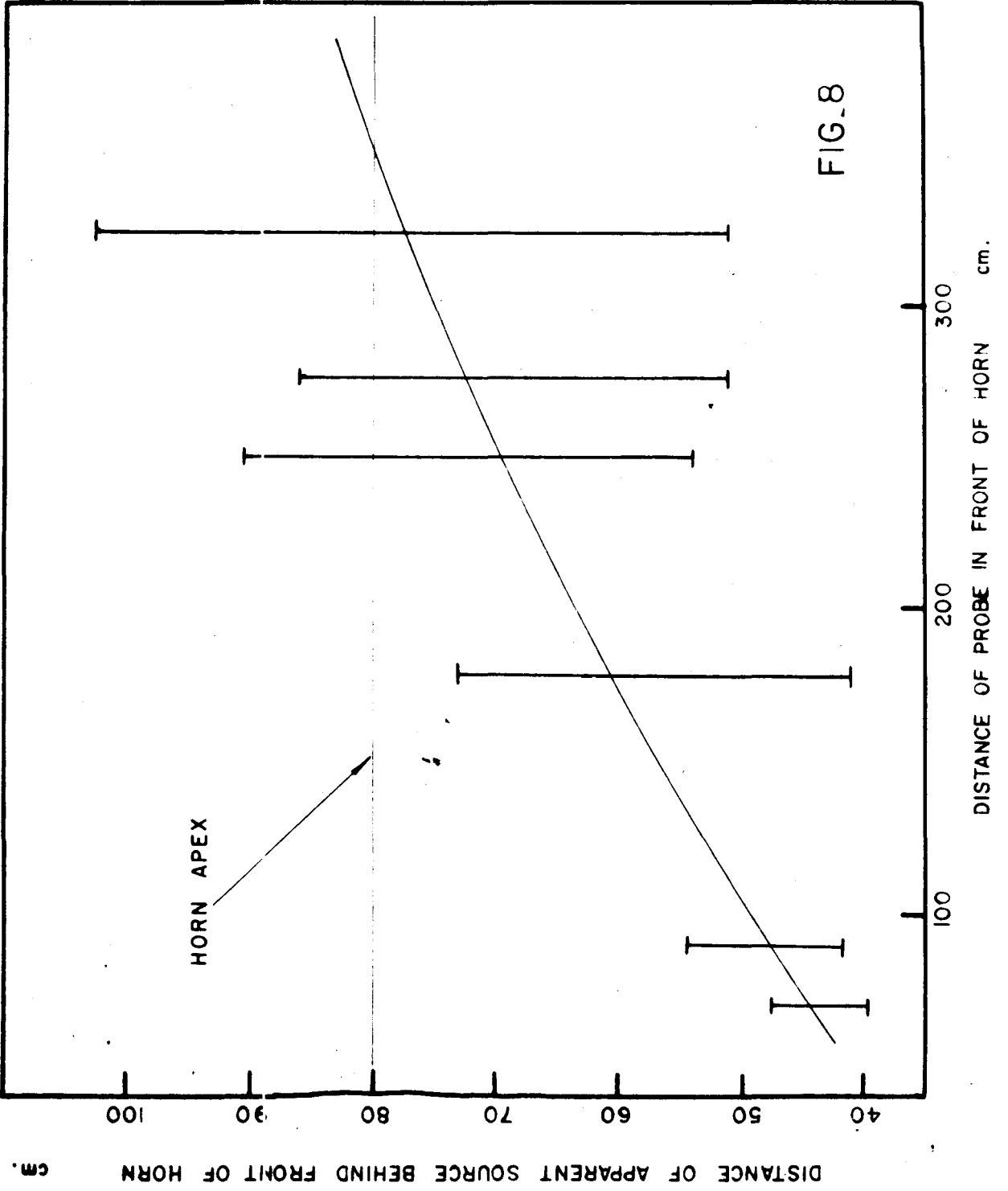probe path tends to increase the errors in phase determina-

FIG_8

DISTANCE OF PROBE IN FRONT OF HORN   cm.

DISTANCE OF APPARENT SOURCE BEHIND FRONT OF HORN   cm.

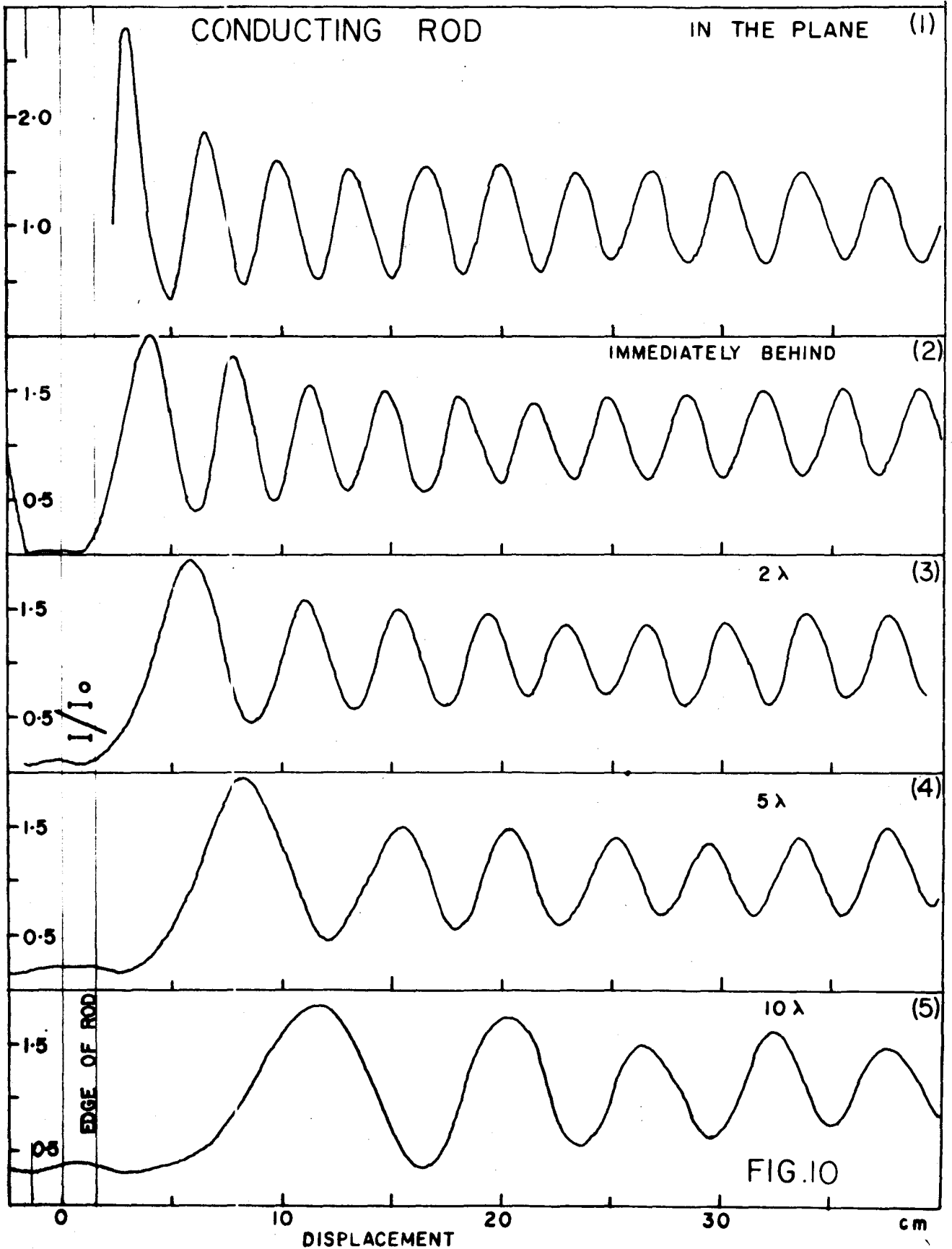HORN APEX

tions at large distances.

However, it would seem that the source is effectively at the apex of the horn for the probe distance of 535 cm used in the following experiments; that the wave fronts are nearly circular and that they may be treated as plane over track runs of the order of 10λ.
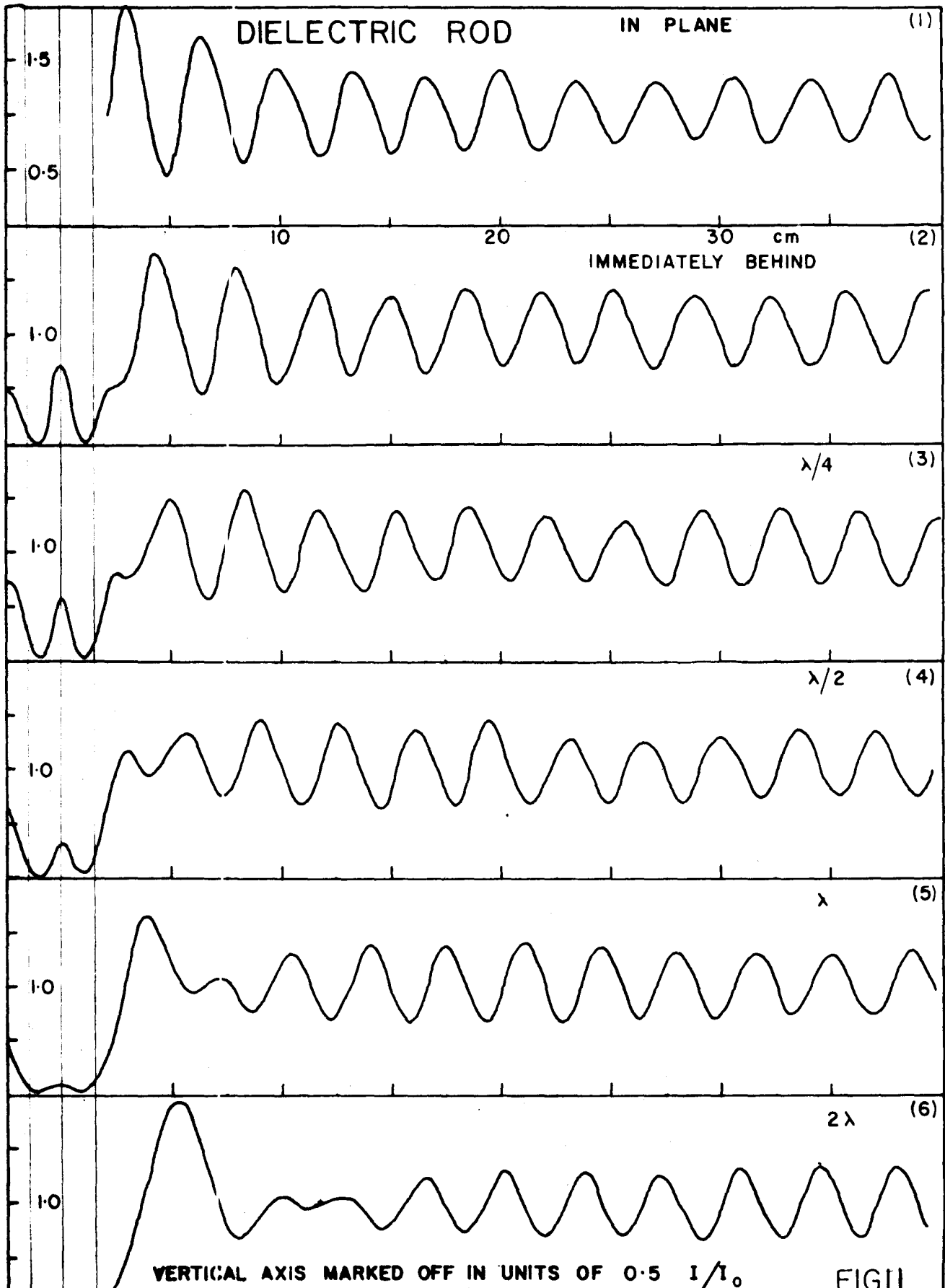
(2) DIFFRACTION BY A CONDUCTING AND NON-CONDUCTING ROD

Following the practice of Stratton and Chu[11] it shall be considered that the x axis is parallel to the E vector (vertical) y parallel to the H vector and Z is along the axis of propogation. The origin will be chosen at the position of the centre of the rod. The track was situated at right angles to the axis of the field (z axis) so that the probe in the centre of the track (y = 0) was located approximately 615 cm (192λ) from the apex of the horn. This distance from the horn was kept constant and the distance of the rod in front of the probe was adjusted for each diffraction run. The hollow brass rod, 57λ long, 0.8λ in diameter and with wall thickness 0.04λ was cleaned, polished and mounted vertically in a wooden block on the floor. The dielectric hard rubber rod, with the same outside dimensions, was cleaned so that a uniform surface was exposed to the radiation, and then mounted in a similar manner. Records of diffraction were made in the plane of the conducting rod (z = 0), immediately behind it (z = 0.629) and at distances 2, 5 and 10λ behind the back edge of the rod, (z = 2.4, 5.4 and 10.4λ) (Fig 10, (1),

(2), (3), (4), (5). Measurements for the dielectric rod were recorded in the plane (z = 0), immediately behind (z=0.629λ) and at distances of $\lambda/4$, $\lambda/2$, and 2λ behind the back edge of the rod (z = 0.65, 0.9, 1.4 and 2.4 λ). Fig 11 (1), (2), (3), (4), (5), (6). The observations were more closely spaced in the dielectric case than in the conducting one because, as will be seen, the interesting effects occur close to the rod.

The following method of taking data was used because the field from the horn at the 535 cm distance extended without undue distortion to a distance of about one meter on each side of the z axis. The variations of intensity of the field were recorded by the Brown recorder from y= 50 cm to y= -10 cm for all other values of z.   The trolley was started at y greater than 50 cm and the recorder chart set in motion just as it passed the 50 cm mark. The trolley was stopped as it passed the y = 2.2 cm or -10 cm mark so that the positions on the chart could be correlated directly with the position of the trolley. The position of the first maximum at y - 3.0 cm was carefully checked and used as a fiducial point for the rest of the pattern. In the cases where the probe could pass behind the rod, the first few peaks on both sides of the centre were obtained and the centre point determined by dividing the distance separating the inside pair by two. Each chart was calibrated by introducing a pip on the pattern with a thump on the table just as the trolley passed a chosen value of y (see Fig 12). After a diffraction experiment with the rod was completed, the re

CONDUCTING ROD

IN THE PLANE (1)

IMMEDIATELY BEHIND (2)

2λ (3)

5λ (4)

10λ (5)

EDGE OF ROD

I/I_0

DISPLACEMENT

FIG.10

DIELECTRIC ROD

VERTICAL AXIS MARKED OFF IN UNITS OF 0·5 I/I_0 FIG11

TYPICAL DIFFRACTION PATTERN
TAKEN FROM RECORDER CHART

Centre
of rod

Disturbed (I)

Undisturbed (I_0)

Calibration
pip
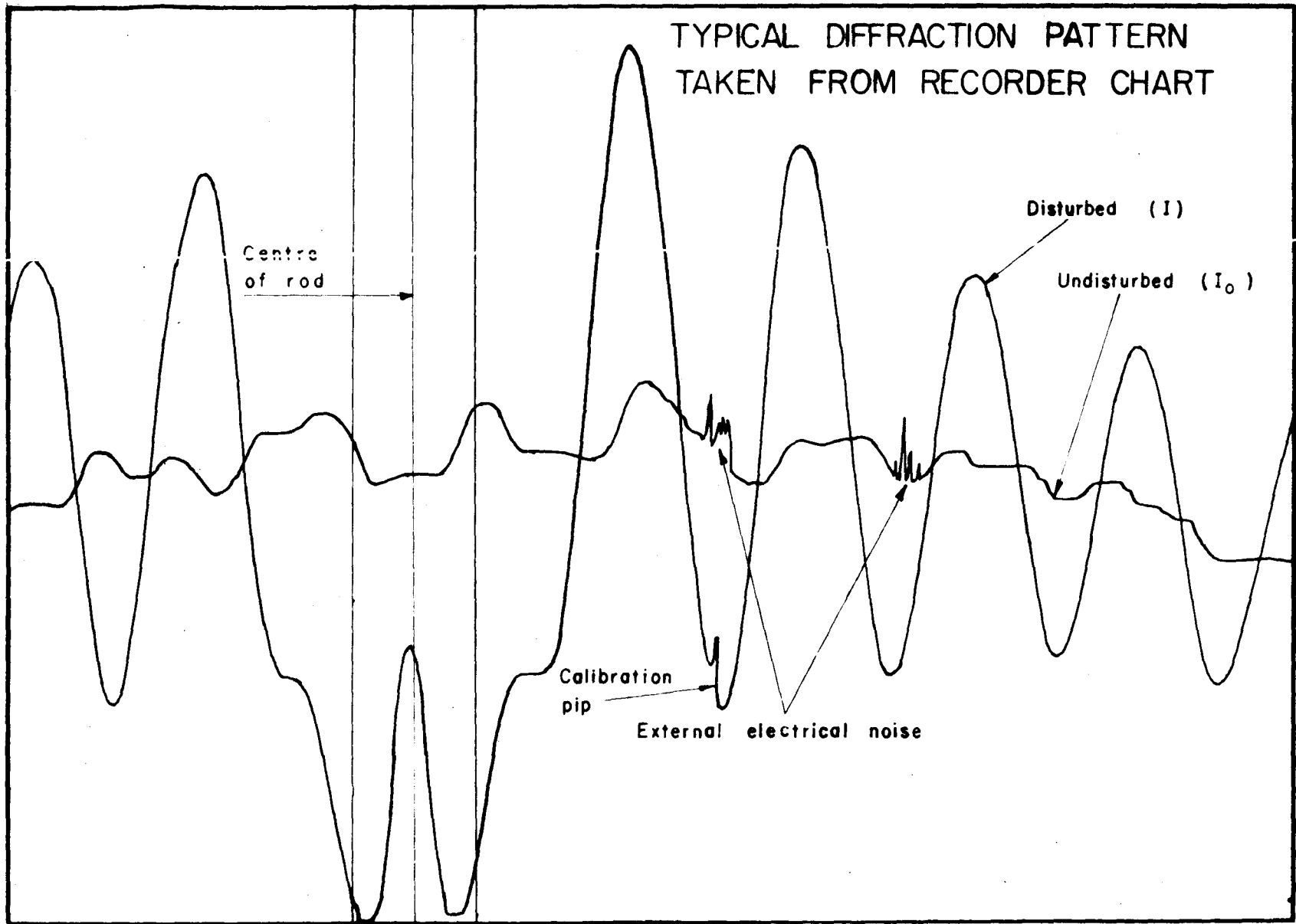
External electrical noise

FIG. 12

corder chart was rewound to the starting point, the rod re-
moved, and the run repeated in the same way. Thus the dis-
turbed and undisturbed patterns were obtained on one record
(fig 12). It is a matter of interest to note by the irregular-
ities on this pattern the presence of stray electrical inter-
ference.

The whole experiment, including runs on both rods
could be carried out in a period of 5 hours, and hence it was
possible to relate the intensities of patterns in the various
cases. When the charts were complete, the distance correspond-
ing to the peak, trough, and one to one points (intersection
of disturbed and undisturbed traces) were measured, converted
to distances on the track and then recorded on the chart it-
self.

Andrews calibrated his crystal detector (IN23A) and
found that "the rectified current through the crystal was
proportional to the square of the potential across it, and
therefore to the rectified power and to the intensity in the
region of the dipole."[7] Since the amplifier is linear, the
amplitude on the chart at any point represents the intensity
I of the field at that point and the ratio I/I_0 of the dis-
turbed to the undisturbed field was easily obtained. Each
such value was recorded opposite its appropriate peak. The
curves I/I_0 vs y are shown in (fig 10 (1), (2), (3), (4),
(5), for the conducting rod and in (fig 11 (1), (2), (3),
(4), (5), (6), for the dielectric rod. The displacements
recorded in the upper right hand corner of each diagram re-

present the distances from the back edge of the rod. To
obtain the z displacement 0.4λ, the radius of the rod, must
be added to each.

(3) INTERPRETATION OF DIFFRACTION RESULTS

Although a number of people have worked in this field,
Kodis,[8] working with 1.25 cm waves is the only one whose
method is close enough of that described in this work to make
comparisons valid. Kodis used a half-plane method which em-
ployed reflection of the antenna and the diffracting rod in a
conducting plane sheet. He gives results of experiment for
both dielectric and conducting rods and the theory for the
latter case. Since, at the time of this writing, the theore-
tical curves applicable to the measurements described in this
thesis are not complete, the results of these experiments can
be compared only qualitatively with those of Kodis. For the
conducting case, the positions of peaks and troughs compare
quite favourably but their shapes differ because Kodis
plotted the amplitude ratio whereas here the intensity ratio
(amplitude [2]) has been plotted. However, a few general re-
marks may be made. The peaks are regular and fall off in
intensity as displacement y increases. In the plane of the
rod, the peaks are uniformly spaced, about 1.07λ apart.
However, the first peak is located, not at $Y = 1.07\lambda$ but at
$y = 0.937\lambda$. As z increases, the amplitude of the first
peaks drops off rather quickly, while that of the more dis-

tant peaks falls off more gradually. The separation of the peaks becomes greater and at $z = 10.4\lambda$, the first peak is located at $y = 3.6\lambda$, and the spacing of successive peaks decreases. This curve also indicates the appearance of a small central maximum in the shadow of the rod. This is shown in the plot of I/I_o presented in Fig 13. This maximum has practically zero intensity close behind the rod, but increases in intensity steadily until it reaches full intensity of the undisturbed field at z approximately equal to 30λ. Only the chief region of interest of z is shown in Fig 13. These measurements have been much more extensive as far as exploration in the y direction is concerned (y up to 12.5λ) than that of other workers and those for large values of y have provided very significant information as will be shown below.

The diffraction curves for the dielectric hard rubber rod differ markedly from those of the conducting case except in the plane ($z = 0$) and at large y. The curves obtained here for $z = 2.4\lambda$ can be compared with one obtained by Kodis for $z = 2.0\lambda$ and there is a definite difference in the results. However this curve (fig 11, (6)) is no doubt qualitatively correct since it is the last of one of a family which exhibit a rapid but regular change with small z (Fig 11, (1), (2), (3), (4), (5), (6), in the vicinity of the vicinity of the rod. Since Kodis obtained patterns only at $y = 2$ and 5λ, he missed the rapid changes in structure which are shown in Fig 11 (1), (2), (3), (4), (5), (6), for small values of z. There is as yet no adequate theory to explain the pattern

FIG.13

DIFFRACTION PATTERNS IN Z AXIS FOR DIELETRIC
AND CONDUCTING RODS 1" IN DIA.
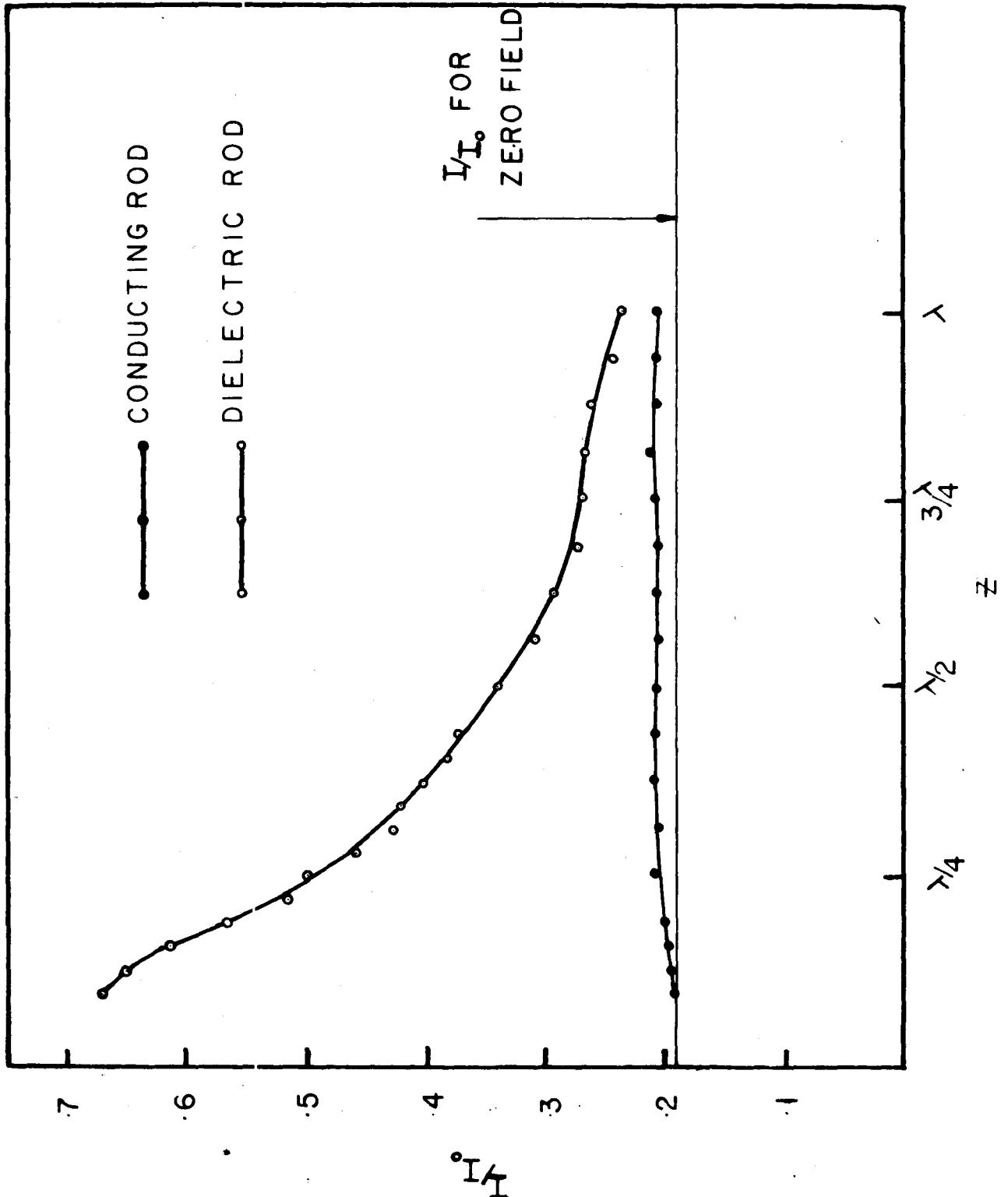
of the dielectric rods.

     The diffraction in the plane of the dielectric rod for y greater than λ is nearly the same as that for the conducting rod as regards peak positions. However, the intensity of the first peak is less than that of the first peak in the conducting case, and the intensities of successive peaks drop off more gradually. The first peak is located at y = 0.937 λ exactly as in the conducting case, and the peak separation is 1.08 λ, nearly the same as of the conducting case. However, at y less than λ for all patterns behind the rod, the similarity ceases. In the first place, the intensity immediately behind the rod is a pronounced maximum (Fig 11 (2)) with $I/I_o \sim 0.7$ and this drops off to zero near z = 2 λ and then increases as z increases (Fig 13). Further, as shown in Fig 11 (2) there is a small partially resolved maximum which increases sharply, becomes resolved and moves out to greater y (Fig 11 (3), (4), (5), (6), as z increases. When z = 2.4 λ, it is much higher than the other peaks in the pattern and is located at y = 1.65 λ. The original first peak of Fig 11 (2) has been decreasing, and as z increases, the second peak is also decreasing. At z = 2.4 λ, these have all but disappeared. These are the main differences in the two patterns. In all cases that can be compared, the patterns for the conducting and dielectric rods are very similar for large y. Fig 14 (1), (2), shows the patterns for z = 0.625 λ of both the dielectric and conducting rods, plotted on the same sheet for purposes of comparison. The theory for the dielectric rod is not
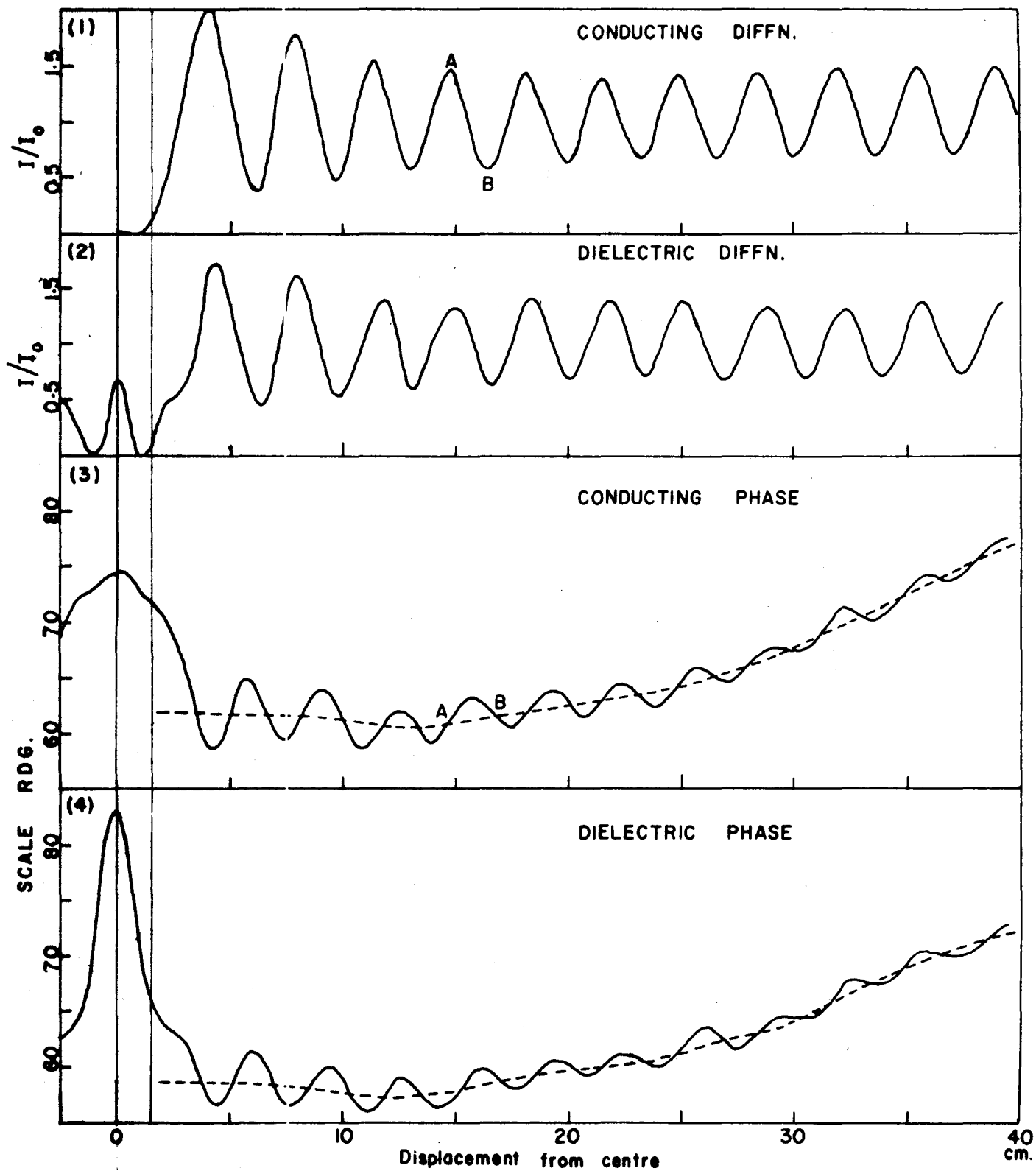
FIG.14

well known and hence, on the basis of theory these anomolies cannot be explained readily. However, on the basis of geo-metrical optics it would seem that the centre peak, immediately behind the rod is due to some focusing effect of the cylinder, acting as a cylindrical lens, which, if the dielectric constant of hard rubber for the wave-length of this radiation is in the correct range, would place the focal point inside the cylinder itself. Further experiments using dielectrics with various values of refractive index might substantiate this idea. Of course, for a lens such as this with aperture of the order of a wave-length, diffraction effects will predominate. This is seen in the whole set of patterns.

(4)   RESULTS OF PHASE MEASUREMENTS

To understand the patterns of phase shown in Fig 14 (3), (4), it is necessary to show the components of the phase of the total field.

If the original cylindrical wave front amplitude is represented by

$$A_z \;=\; Ce^{i\,(yz)} \;=\; C\,(\cos\phi + i\,\sin\phi)$$

where c is a constant   and $\phi = \dfrac{2\pi\ell}{\lambda}$ (Fig 15).

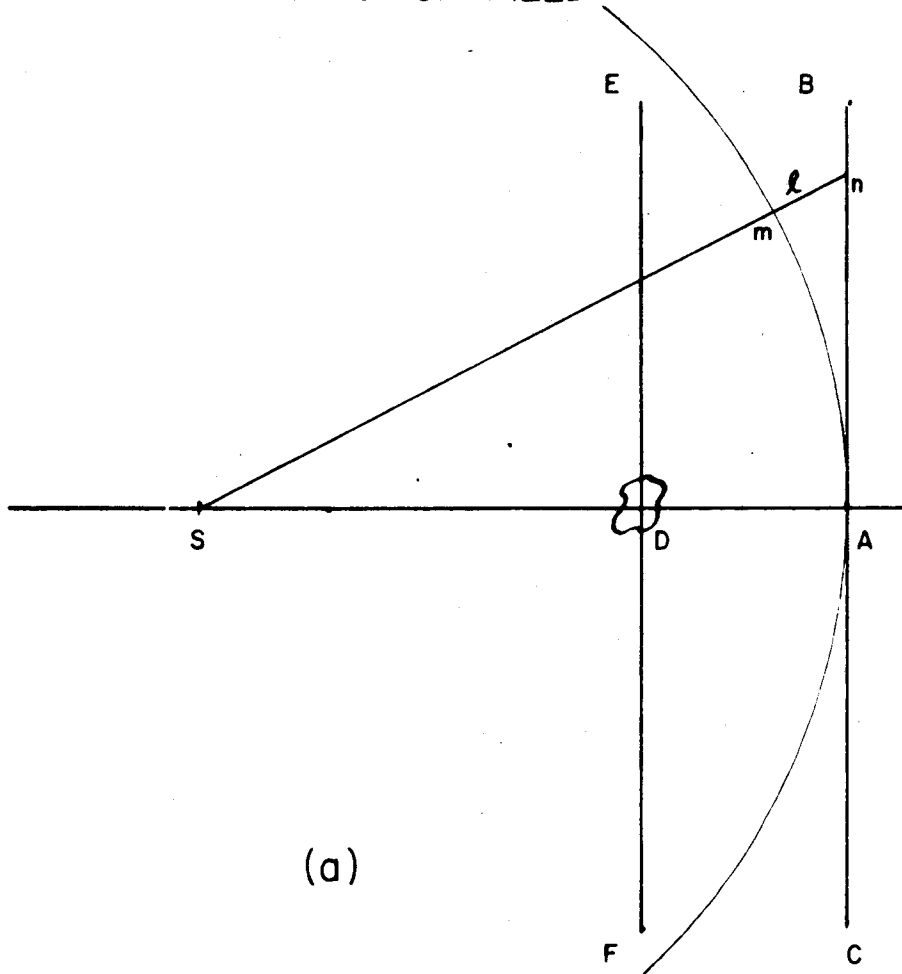The amplitude squared is
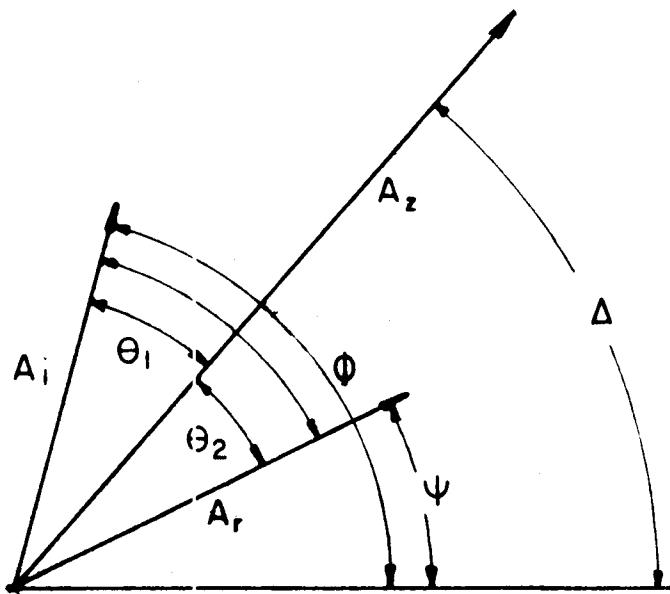
$$A_z^2 \;=\; \cos^2\phi + \sin^2\phi$$

and

$$\tan \;=\; \frac{\sin\phi}{\cos\phi}$$

Hence ϕ represents the phase of the field relative

PHASE Φ OF FIELD

(a)

(b)

FIG. 15

PHASE COMPONENT RELATIONS

to the ideal plane wave C A V (Fig 15). When an obstacle is located at D, the field consists of two parts

A_i, the indicent field and

A_r, the re-radiated field.

The point of discussion is y, z.

$$A_z = A_i + A_r = c\,e^{i\phi(yz)} + \text{(terms due to re-radiation)}$$

$$A_z = (C\cos\phi + \textstyle\sum \text{real terms})$$

$$i\,(C\sin\phi + \textstyle\sum \text{real terms})$$

and

$$\tan\Delta = \frac{\sin\phi - \sum \text{real terms}}{\cos\phi - \sum \text{real terms}} \qquad - 3$$

where Δ is the phase of the combined fields at the point (y,z) Call the phase of the re-radiated component Ψ. Then if the sums given in 3 above can be evaluated, the magnitude and direction of the resultant and re-radiated components may be obtained experimentally. Thus the problem is known.

Then

$$\vec{A_z} = \vec{A_i} + \vec{A_r}.$$

Then, with reference to Fig 15 (b)

$$A_r^2 = A_i^2 + A_z^2 - A_i A_z \cos\theta 1.$$

Therefore $$\cos\theta 1 = \frac{A_i^2 + A_z^2 - A_r^2}{2A_i\,A_z}$$

or $$A_i^2 = A_r^2 + A_z^2 - 2A_r A_z \cos\theta_2$$

and $$\cos\theta_2 = \frac{A_r^2 + A_z^2 - A_i^2}{2A_r A_z}$$

Thus, from Fig 15 (b)

$$\Delta = \phi - \cos^{-1} \frac{A_i^2 + A_z^2 - A_r^2}{2 A_i A_z}$$

or

$$\Delta = \psi + \cos^{-1} \frac{A_r^2 + A_z^2 - A_i^2}{2 A_r A_z}$$

where

Δ is the phase of the total combined pattern relative to CAB,

ϕ is the phase of the incident field relative to CAB,

ψ is the phase of the re-radiated field relative to CAB,

δ is the difference in phase of A_i and A_r.

Qualitatively the picture looks like this. The phase ϕ represents the distance $2\frac{\pi \ell}{\lambda}$ through which the wave must travel, from the wave front to the line CAB, which represents the plane through which the probe moves. In other words, each ray from the source must travel over a longer path length as the displacement of the probe from A increases. Thus the phase of the wave at any given point on CAB lags in phase with respect to a point lying closer to A. This phase is shown by the dotted curve in Fig 14 (4), (5). The vector A_i on Fig 15 (a) defines ϕ from the zero reference line (phase at A) and as Y increases from 0 to 15λ say, ϕ will increase from 0 to 180° lag. The vector A_z represents the radiated field and its phase is given by ψ. As ϕ increases, ψ increases rapidly and will complete one cycle of phase (360° lag) in approximately one wave-length of path travelled by the probe. Now, the resultant field, A_z, will be a maxi-

mum when $\phi = \psi$, ($\delta = 0$) and hence when A_i and A_r are directed in the same direction, and A_z will be a minimum when A_i and A_r are directed in the opposite sense, that is, when $\phi = -\psi$ ($\delta = 180°$). This fact is shown in Fig 14 (3) (4). (conducting and dielectric phases respectively). The argument holds for both rods and only the conducting rod will be considered.

Point A on Fig 14 (1) represents a maximum in the diffraction pattern. Corresponding to that point, A on Fig 14 (3) represents a point where the resultant phase intersects the ϕ curve, thus indicating $\delta = 0$. The points B, for the minimum on the diffraction curve are given when the resultant phase goes through one cycle and intersects again the ϕ curve. Hence $\delta = 180°$ and this corresponds to a minimum on the intensity curve (Fig 16 (1)).

However, the phases for y less than 1.6λ do not obey this argument, and each case must be treated separately. Consider the contribution to A_r as a series of rays arriving from the source along the plane F D E and proceeding from there by further Huyghens' wavelets to the point under consideration on C A B. These rays travelling through the points on F D E more remote from D will lag more in phase than those rays travelling by a more direct route. Also the more direct rays contribute more to the resultant intensity because they are larger in amplitude. If these direct rays are cut out as in the case for points on CAB immediately behind the rod, the net result will be a phase which lags the zero phase of the

incident field. This is shown by the central hump on Fig 14 (3). In the dielectric case, energy is obtained through the rod and this argument no longer holds. It is observed from Fig 14 (4) that the radiation arriving at points immediately behind the dielectric rod arc lagging in phase with respect to the incident field. The energy suffers, as it were, a phase shift in passing through the rod.

Quantitative measurements of phase are difficult. The apparatus is so arranged that the phase indication at A is a minimum and the probe is run over a sufficiently large distance so that a maximum which gives an indication of $\phi = 180°$ will appear. Thus the $\phi = 0$ and $\phi = 180°$ points are known and the scale of relative phase is established. However, limitation of track length in the Y direction for such large distances from the source did not allow for more than those shown. Estimates only of the phase limits can be made by extrapolation. For the conducting case, $\phi = 0$ corresponds to a scale reading of 62 and $\phi = 180°$ corresponds to 85 units of scale. For the dielectric cases $\phi = 0$ is given by a scale reading 59 and $\phi = 180°$ is given by scale reading 82. On the whole these phase results are of qualitative interest only, the measurements of intensities and positions of peaks, being of much greater importance in the diffraction problem.

TYPICAL FIELD PHASE RECORD

(b)

-32-
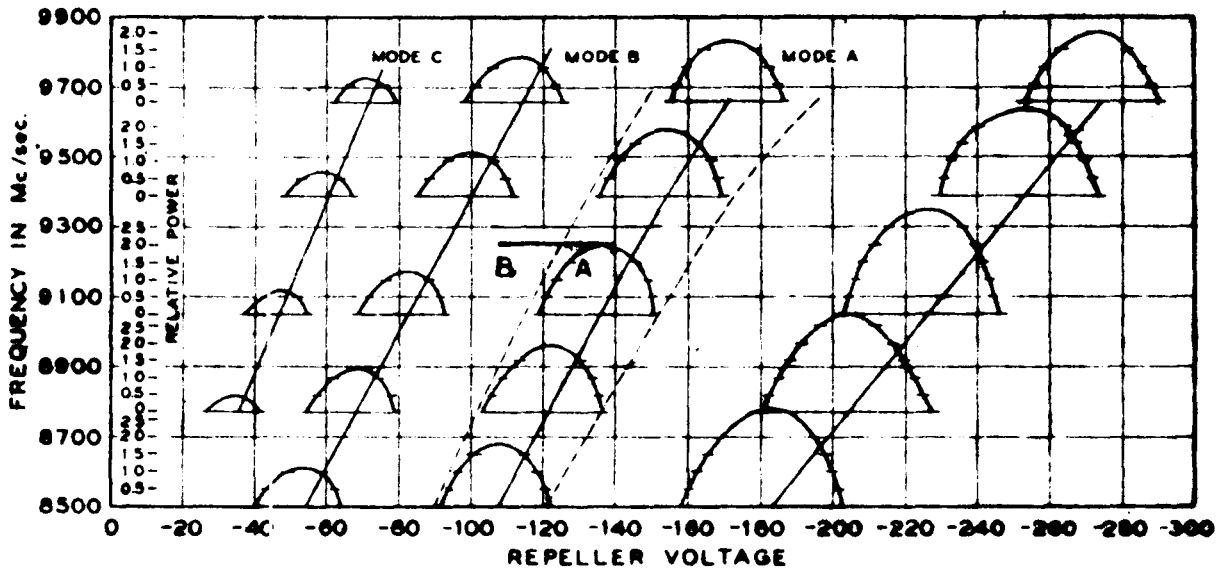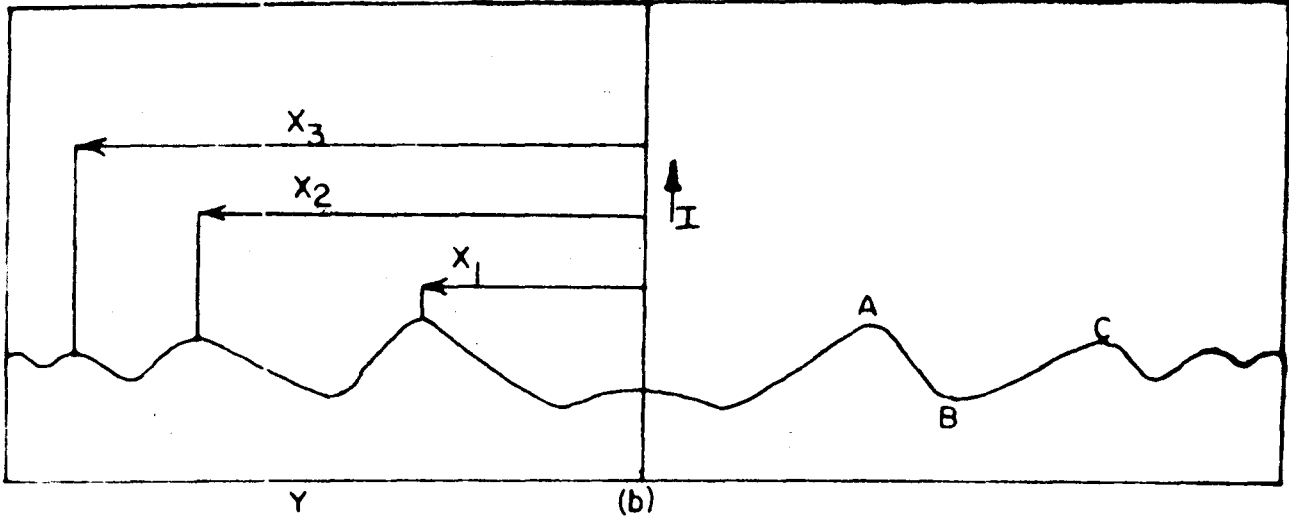
CONCLUSION

The study of diffraction about the rods described in this thesis agree with those of Kodis for the conducting case. The dielectric diffraction results, however, differ from Kodis. They show interesting properties of the dielectric rod which may be considered as a special case of an infinitely long cylindrical lens with aperture of the order of one wave-length. The outstanding difference between these two cases of diffraction occur at small (2 or 3 wave-lengths) lateral displacements at right angles to both E and H vectors. The similarity of the "dielectric" and "conducting" patterns is shown by the respective peak and trough positions for large lateral displacements.

These studies have been made with the field polarized so that the E vector was parallel to the axis of the rod. A complete set should be carried out with the E vector perpendicular to the axis of the rod since the theory for this case is unknown.

One weakness in this experimental setup occurred in the uncertainty in locating the track in the field at various distances along and at right angles to the axis of the field. Improvement could be made by placing the track on graduated rails, parallel to the axis of propagation, so that each point in the field could be determined exactly.

The radiation scattered from the boundaries of the room contributed irregular disturbances to the so called undisturbed pattern. Careful attempts should be made to

reduce this standing wave ratio, which imposed a limitation on the range of the lateral displacements. This limitation was obvious from the same relative sizes of the variations of the "disturbed" and "undisturbed" traces for displacements from the rod greater than about 14 wave-lengths.

It is recommended that the linearity of the amplifier be investigated. Good linearity is necessary to allow more exact measurements of I/I_o .

REFERENCES

No.	Ref.
11.	J. A. Stratton & L.J. Chu, Phys. Rev., 56, 105, (1939)
7.	C.L. Andrews, Phys. Rev., 71, 777 (1947)
8.	R. D. Kodis, J. Appl. Phys., 23, 249, (1952)
3.	C.G. Montgomery, : Technique of Microwave Measurements, Vol 9, Radiation Laboratory Series: McGraw-Hill,(1947)

BIBLIOGRAPHY

D. B. McLay, Thesis for Degree Master of Science, McMaster, (1951)

J. C. Slater and N. H. Frank, Electromagnetism (New York, McGraw-Hill, 1947)

Massachusetts Institute of Technology Radiation Laboratory Series (New York, McGraw-Hill)

> Vol. 11   C. G. Montgomery, Technique of Microwave Measurements (1947)

> Vol. 12   S. Silver, Microwave Antenna Theory and Design (1949)

> Vol. 15   H. C. Torrey and C. A. Whitmer, Crystal Rectifiers (1948)

> Vol. 23   S. N. Van Voochis, Microwave Receivers (1948)

J. A. Stratton, Electromagnetic Theory (New York, McGraw-Hill, 1941)

D. W. Fry and F. K. Goward, Aerials for Centimetre Wave-Lengths (Cambridge University Press, 1950)

C. L. Andrews, Phys. Rev., 71, 777 (1947)

R. D. Kodis, J. Appl. Phys., 23, 249 (1952)

P.M.Morse, Vibration and Sound (McGraw-Hill, New York 1936)

C. L.Andrews, J. Appl. Phys., 21, 764 (1950)

J. A. Stratton and L.J. Chu, Phys. Rev., 56, 105 (1939)